J Nanotechnol Res 2022; 4 (2): 31-44 *DOI: 10.26502/ jnr.2688-85210029*

Research Article

From Waste Tea to Carbon Rocket Fuels through a Piranha Solution-Mediated Carbonization Treatment

Georgios Asimakopoulos[1], Dimitrios Moschovas[1], Apostolos Avgeropoulos[1], Athanasios B Bourlinos[2*], Iosif Tantis[3], Veronika Sedajova[3,4], Ondrej Tomanec[3], Constantinos E Salmas[1], Dimitrios Gournis[1], Michael A Karakassides[1]

[1]Department of Materials Science and Engineering, University of Ioannina, 45110 Ioannina, Greece

[2]Physics Department, University of Ioannina, 45110 Ioannina, Greece

[3]Regional Centre of Advanced Technologies and Materials, Czech Advanced Technology and Research Institute (CATRIN), Palacky University, Slechtitelů 27, Olomouc, 78371, Czech Republic, Czechia

[4]Department of Physical Chemistry, Faculty of Science, Palacký University, 17. Listopadu 1192/12, Olomouc, 77900, Czech Republic, Czechia

[*]Corresponding author: Athanasios B Bourlinos, Physics Department, University of Ioannina, 45110 Ioannina, Greece. Tel: +302651008511

Received: 07 April 2022; **Accepted:** 18 April 2022; **Published:** 19 April 2022

Citation: Georgios Asimakopoulos, Dimitrios Moschovas, Apostolos Avgeropoulos, Athanasios B Bourlinos, Iosif Tantis, Veronika Sedajová, Ondrej Tomanec, Constantinos E Salmas, Dimitrios Gournis, Michael A Karakassides. From Waste Tea to Carbon Rocket Fuels through a Piranha Solution-Mediated Carbonization Treatment. Journal of Nanotechnology Research 4 (2022): 31-44.

Abstract

In a previous work we have demonstrated the carbonization of biomass waste, such as stale bread, spent coffee and cardboard, in piranha solution towards the formation of hypergolic carbons that could be exploited as solid fuels in rocket engines. These cases simply aimed to provide some interesting examples of waste valorization towards a new class of carbon-based rocket fuels rather unique to the piranha solution treatment. In an effort to further strengthen this concept with additional examples herein we report the carbonization of waste tea in piranha solution towards the formation of hypergolic carbons at decent yield. Likewise bread, coffee and

cardboard waste, spent tea is also produced in large quantities worldwide every year, thus meriting further attention in this context. Consistently with the previously reported results, the piranha solution-mediated carbonization of waste tea produces carbon nanosheets that spontaneously ignite upon contact with fuming nitric acid HNO_3 at ambient conditions. Interestingly, intercalation of the nanosheets with certain ignitable molecules further boosts carbon hypergolicity upon contact with fuming nitric acid HNO_3. These findings come to confirm the versatile character of the method in diverting biomass waste into valuable energetic carbons by piranha solution.

Keywords: Biomass waste; Carbonization; Carbon nanosheets; Hypergolic carbon; Piranha solution; Rocket fuels; Waste tea; Waste valorization

1. Introduction

Nowadays biomass waste is increasingly growing as a result of intense human activity to meet ever expanding needs of our modern society. This sizeable amount of waste eventually piles up and rots in landfills thus posing severe threats for the environment due to extensive putrefaction. Accordingly, there is a burgeoning interest in converting biomass waste into a valuable source of energy, chemicals, absorbents, fertilizers and functional carbon materials [1]. In this latter context, our group has recently shown that biomass waste carbonization in piranha solution is a versatile new method for obtaining hypergolic carbons suitable for solid rocket fuels [2], thus providing an unusual example of biomass waste valorization rather unique to the piranha solution treatment. To that aim, stale bread, spent coffee and cardboard wastes were chosen as examples, all discarded in landfills in large quantities without further processing. Interestingly, the obtained carbons reacted hypergolically upon contact with fuming nitric acid HNO_3 at ambient conditions, whereas intercalation with ignitable molecules (e.g., aniline) further boosted carbon hypergolicity towards faster and brighter ignitions [2]. Tea is a popular beverage with nearly 6 million tons consumed across the world yearly. As a consequence, tea creates a considerable amount of biomass waste that can raise serious environmental issues. As a result, a lot of scientific effort is devoted on finding practical ways to deal with this waste. Certain efforts pertain to the production of energy, the extraction of valuable chemicals, biogas generation, natural adsorbents and fertilizers [3-9]. Waste tea additionally serves as the starting material for the pyrolytic synthesis of functional carbon materials suitable for supercapacitors, fluorescent nano-sensors or adsorbent materials [10-15]. However, no report in the literature refers to the carbonization of waste tea in piranha solution. Due to a mass production, waste tea undoubtedly merits further consideration in this token. In an effort to extent this concept to sizeable biomass wastes other than stale bread, spent coffee and cardboard; herein we present the carbonization of waste tea in piranha solution towards the formation of carbon nanosheets at good yield. As it has been previously demonstrated for the stale bread-, spent coffee- and cardboard-derived carbons, the waste tea-derived carbon also reacts hypergolically with fuming nitric acid HNO_3 at ambient conditions giving bursts of yellow flame upon contact with the strong oxidizer. Such spontaneous ignition seems pretty specific to the piranha solution treatment and can hardly be seen for pyrolytically-derived carbons. Worth noting, intercalation of certain ignitable molecules between

the nanosheets, such as aniline, furfuryl alcohol and hydrazine, further boosts carbon hypergolicity with fuming nitric acid HNO_3. Overall, biomass waste carbonization in piranha solution appears to be a general new method towards the fabrication of hypergolic carbons well suited as power sources in rocket propellants.

2. Materials and Methods

Synthesis was conducted in a fume hood. Concentrated H_2SO_4 98 % and H_2O_2 30 % were supplied by Merck. Piranha solution is highly corrosive and should be handled with great care. Waste tea was obtained from used tea bags (brand name DIPLOMAT®, Gold BLEND, Black Tea) after drying. Typically, 40 g waste tea were poured into a beaker containing 100 mL piranha solution (3:1, 75 mL H_2SO_4 98 %-25 mL H_2O_2 30 %) as shown in (Figure 1). The fast (within 10-15 min) and exothermic reaction that took place led to complete carbonization of the waste tea by concurrent formation of CO_2 gas bubbles and hot steam vapor (H_2O). The carbonized product was rinsed several times with water until neutral pH, with acetone until no coloration of the solvent was observed and with Dimethyl Form Amide (DMF, Sigma-Aldrich) until no coloration of that solvent was observed. After rinsing with DMF, the sample was once again rinsed with water and acetone in order to remove the polar solvent, air-dried at 100 ^oC and crushed into a fine black powder at yield 32 % (specific surface area from N_2 BET was 1-5 m^2 g^{-1}). The sample is thereafter denoted as WTPS (from **W**aste **T**ea-**P**iranha **S**olution).

Figure 1: From left-to-right: waste tea carbonization in piranha solution, followed by washing and drying of the product, resulted in a fine carbon powder (namely WTPS) at 32 % yield.

The aniline, furfuryl alcohol and hydrazine intercalates of WTPS were obtained as following: 2 g of WTPS were respectively mixed with 2 g of aniline or furfuryl alcohol or hydrazine hydrate (Sigma-Aldrich) in a sealed glass vial to form wet pastes. The wet pastes were placed at 100 °C for a day in an oven in order to force the intercalant molecules into the gallery space of carbon towards the formation of the corresponding aniline-, furfuryl alcohol- and hydrazine-intercalated adducts in the form of dry black powders. X-Ray Diffraction (XRD) was conducted on background-free holders using Co Kα radiation from X`Pert PRO diffractometer (Malvern Panalytical) operating in Bragg-Brentano geometry. Raman spectrum was recorded with a micro-Raman system RM 1000 Renishaw using a laser excitation line at 532 nm. Atomic Force Microscopy (AFM) images were collected on silicon wafers in tapping mode with a Bruker Multimode 3D Nanoscope (Ted Pella Inc., Redding, CA, USA). Scanning Electron

Microscopy (SEM) images were obtained using a JEOL JSM-6510 LV SEM Microscope (JEOL Ltd., Tokyo, Japan) equipped with an X-Act EDS-detector by Oxford Instruments (Abingdon, Oxfordshire, UK, an acceleration voltage of 20 kV was applied). For the Transmission Electron Microscopy (TEM) study, a JEOL 2010 instrument, equipped with a LaB_6 type emission gun operating at 160 kV (JEOL Ltd., Tokyo, Japan) was used. Energy-Dispersive X-Ray Spectroscopy (EDS) was recorded on an Oxford x-MAX 80T (SSD) at 200 kV accelerating voltage. Scanning transmission electron microscopy high-angle annular dark-field (HAADF) imaging analyses for EDS mapping of elemental distributions on the products were performed with an FEI Titan HRTEM microscope operating at 80 kV. X-Ray Photoelectron Spectroscopy (XPS) was performed with a PHI VersaProbeII (Physical Electronics) spectrometer using an Al Ka source (15 kV, 50 W). The obtained data were evaluated and deconvoluted with the MultiPak (Ulvac - PHI, Inc.) software package. The spectral analysis included Shirley background subtraction and peak deconvolution employing mixed Gaussian-Lorentzian functions.

3. Results and Discussion

3.1. Structure and morphology of WTPS

The XRD pattern of WTPS (Figure 2, top) shows a very broad (002) reflection with an interlayer spacing of d_{002} = 4.5 Å that is considerably larger than that of crystalline graphite with d_{002} = 3.4 Å [16]. The broadness of the reflection along with the relatively high d_{002} value pinpoints the formation of amorphous, highly disordered carbon [17, 18]. The small sharp reflection near $2\theta = 30^{o}$ is assigned to residual calcite $CaCO_3$ phase. Raman spectroscopy (Figure 2, bottom) shows the characteristic D and G bands at 1377 and 1587 cm^{-1}, respectively, with an intensity ratio I_D/I_G = 0.49, also indicative of amorphous carbon [17-19]. Furthermore, the strong yet broad band centered at 2944 cm^{-1} can either be attributed to nitrogenous carbon [20] or/and to a set of broad and superimposed D + D", 2D, D + G and 2D' bands due to incompletely crystallized graphite-like carbon [16].

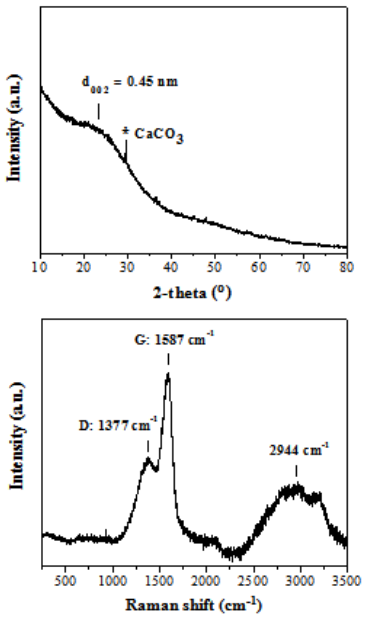

Figure 2: XRD pattern (top) and Raman spectrum (bottom) of WTPS.

The elemental composition and chemical state of WTPS was analyzed through the XPS technique. In the survey spectra (Figure 3, top) the presence of C (70.3 %) and O (25.1 %) is dominant with low amounts of Ca (0.9 %), S (1.7 %) and N (2 %), as expected from the chemical composition of waste tea [21] as well as the piranha solution processing that may result in sulfur incorporation into the carbon lattice. The oxidized state of carbon, which explains the high presence of oxygen at the survey spectra, was further evidenced in the high-resolution C 1s XPS profile (Figure 3, bottom). Thus, the characteristic peaks for oxidized carbon are present with the deconvoluted C1s peaks corresponding to sp^2/sp^3 carbons (284.8 eV, 58.7 %), C-O (286.1 eV, 23.5 %), C=O (287.4 eV, 9.5 %) and O-C=O (289.1 eV, 6.8 %) [22]. The component at 291.3 eV corresponds to the characteristic satellite feature, ascribed to the $p\text{-}p^*$ transition appearing at sp^2 conjugated carbons [23].

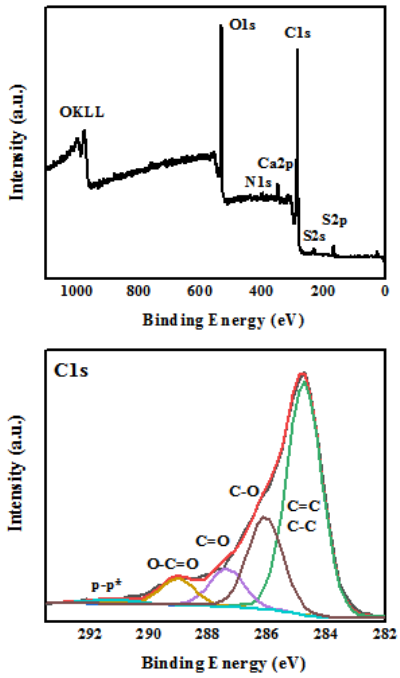

Figure 3: XPS survey (top) and deconvoluted C1s (bottom) spectra of WTPS.

The morphology of WTPS was assessed by SEM and TEM electron microscopies. SEM shows nanosheets consisting of stacked quadrangle plates with lateral dimensions 2-10 μm, as well as, larger flakes of various shapes bigger than 10 μm (Figure 4).

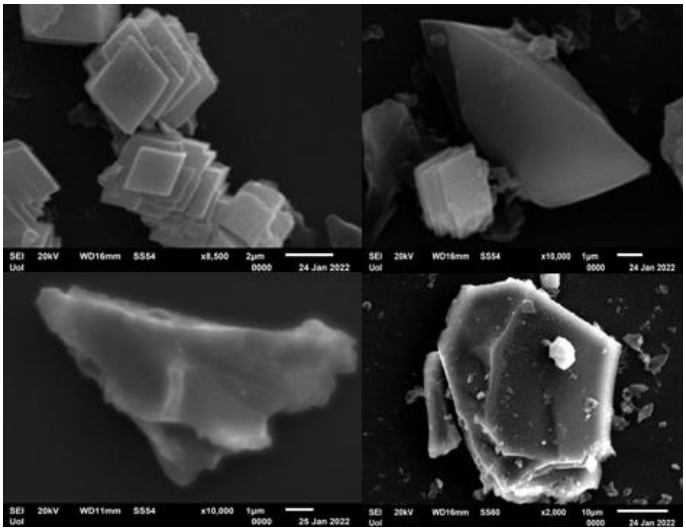

Figure 4: SEM images of WTPS.

In line with SEM, TEM also confirms the presence of large nanosheets with smooth surface exhibiting a multilayer texture near the edges due to the phylomorphous structure of the solid (Figure 5).

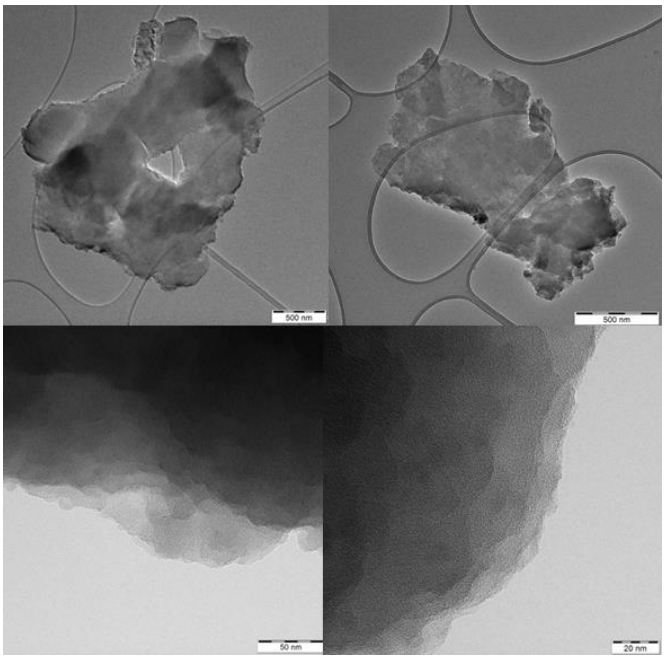

Figure 5: TEM images of individual carbon nanosheets (top) showing multilayer texture near the edges (bottom).

From the height profiles of the AFM inspection (Figure 6), the nanosheets appear to consist of both thin sheets with thickness 1-2.5 nm and thick sheets with thickness 2.5-35 nm.

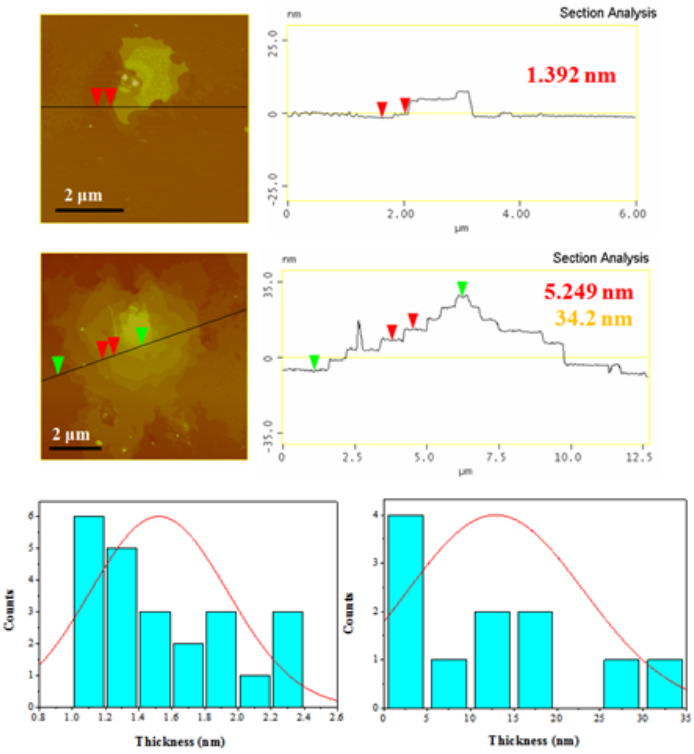

Figure 6: AFM images of cross-sectional analysis of selected sheets and statistical analysis histograms of thinner (1-2.5 nm, left) and thicker (2.5-35 nm, right) sheets.

On the other hand, chemical mapping (Figure 7), addressed by energy-dispersive X-ray spectroscopy using HR-TEM, revealed a homogeneous distribution of the XPS-detected C, O, N and S elements in the sample, thus confirming an even chemical composition for WTPS.

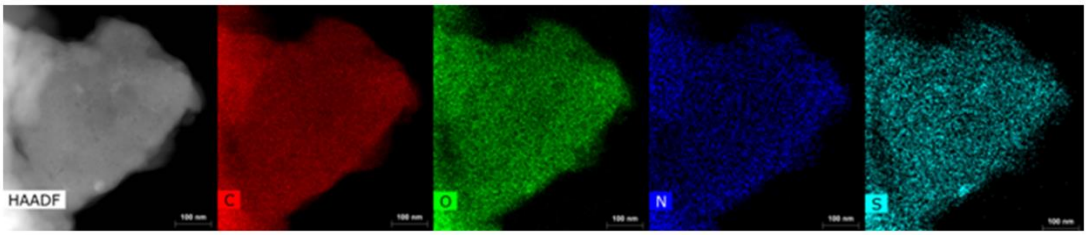

Figure 7: HR-TEM chemical mapping of WTPS (scale bar 100 nm). Red denotes C, green O, blue N and light blue S.

3.2. Hypergolicity of WTPS

In hypergolic propellants a fuel and a strong oxidizer ignite fast and spontaneously upon contact at ambient conditions to provide the necessary energy needed to lift-off space rockets. Certain standards for an employed fuel are high energy value, high density

(*e.g.*, solid fuels), low cost, low toxicity and fast ignition upon contact with the strong oxidizer. Several combinations of fuel-oxidizer exist today to serve this purpose but none of them exploits carbon as fuel. Although carbon is of relatively high energy value and density as well as of low cost and toxicity, its usage as rocket fuel is underexplored [2, 24, 25]. A possible reason for this might be the fact that carbon is kinetically difficult to spontaneously ignite at ambient conditions, mainly due to limited access of a strong oxidizer to the basal plane of the layered carbon, thus inhibiting a fast exothermic reaction. One way to deal with this problem is to structurally engineer carbon so as to display a large interlayer spacing that will allow the molecules of the strong oxidizer to easily access the gallery space of carbon and trigger a fast and spontaneous exothermic reaction. This is actually the case for the carbons obtained from biomass waste carbonization in piranha solution, where the in-situ liberation of hot CO_2 gas helps to push the carbon layers apart from each other, thus creating a relatively large interlayer spacing (d_{002} > 4 Å) [2]. In the present case and likewise the stale bread-, spent coffee- and cardboard-derived hypergolic carbons discussed elsewhere [2], the carbon obtained from piranha solution treatment of waste tea also displays a large interlayer spacing and, as such, it reacts too hypergolicly when comes in contact with fuming nitric acid HNO_3 (Figure 8).

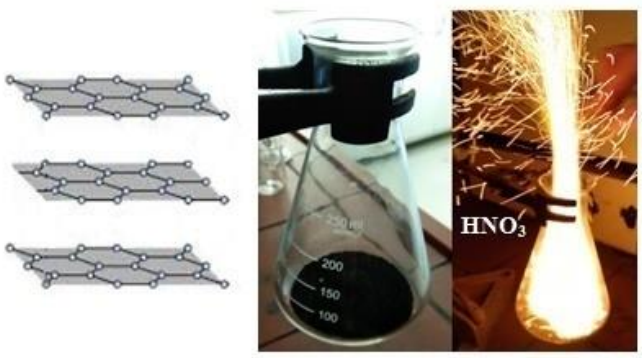

Figure 8: The addition of fuming nitric acid HNO_3 to WTPS layered carbon leads to hypergolic ignition at ambient conditions.

Specifically, the addition of 5 mL fuming nitric acid HNO_3 (100 % Merck) to 4 g WTPS resulted in spontaneous ignition at ambient conditions. Since the average size of HNO_3 is about 3.5 Å, the molecules of the strong oxidizer fit in the interlayer space of carbon as shown in (Figure 9). Therefore, the strong oxidizer can easily access the basal plane of the carbon lattice to trigger ignition according to the exothermic reaction:

$$5\ C + 4\ HNO_3 \rightarrow 2\ N_2 + 5\ CO_2 + 2\ H_2O\ \Delta H = -1626\ kJ$$

Worth noting, crystalline graphite (Alfa Aesar), charcoal (Merck) and active carbon (Aldrich) with d_{002} values between 3.4 and 3.6 Å *(i.e.*, more or less close to the size of HNO_3) gave no ignition upon contact with the strong oxidizer due to limited intercalation of the HNO_3 molecules into the gallery space of the corresponding carbons. Since synthetic graphite, charcoal and active carbons are obtained *via* pyrolytic methods, these control experiments highlight the importance of the piranha solution treatment in obtaining ignitable carbons with large interlayer spacing (d_{002} > 4 Å) not achievable through pyrolytic methods (d_{002} < 4 Å).

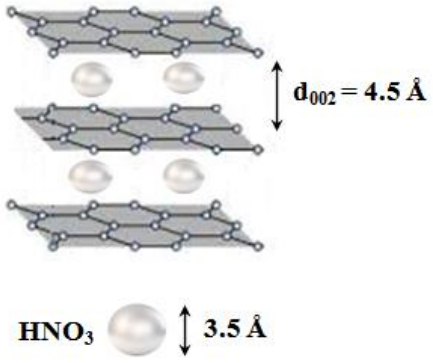

Figure 9: Schematic representation of HNO_3 intercalation into the gallery space of carbon. Once HNO_3 reaches the carbon basal plane, this triggers ignition according to the reaction presented above.

In addition, the ignition was found to be sensitive to the amount and ratio of the mixed reagents, in accordance with previous observations on the ignition behavior of the stale bread-, spent coffee- and cardboard-derived carbons against fuming nitric acid HNO_3 [2]. In order to overcome this problem, the nanosheets were intercalated with small ignitable molecules, such as aniline, furfuryl alcohol and hydrazine, all known to react hypergolicly against fuming nitric acid HNO_3 [26-28]. Characteristically, the addition of HNO_3 to the aniline-, furfuryl alcohol- and hydrazine-intercalated WTPS adducts prepared according to the experimental section, gave fast and bright ignitions irrespectively of the amount and ratio of the mixed reagents (Figure 10). These results indicate that tailoring of the gallery space of the derived carbons with hypergolically active molecules can further boost carbon hypergolicity, as it is highly deemed for rocket propellants.

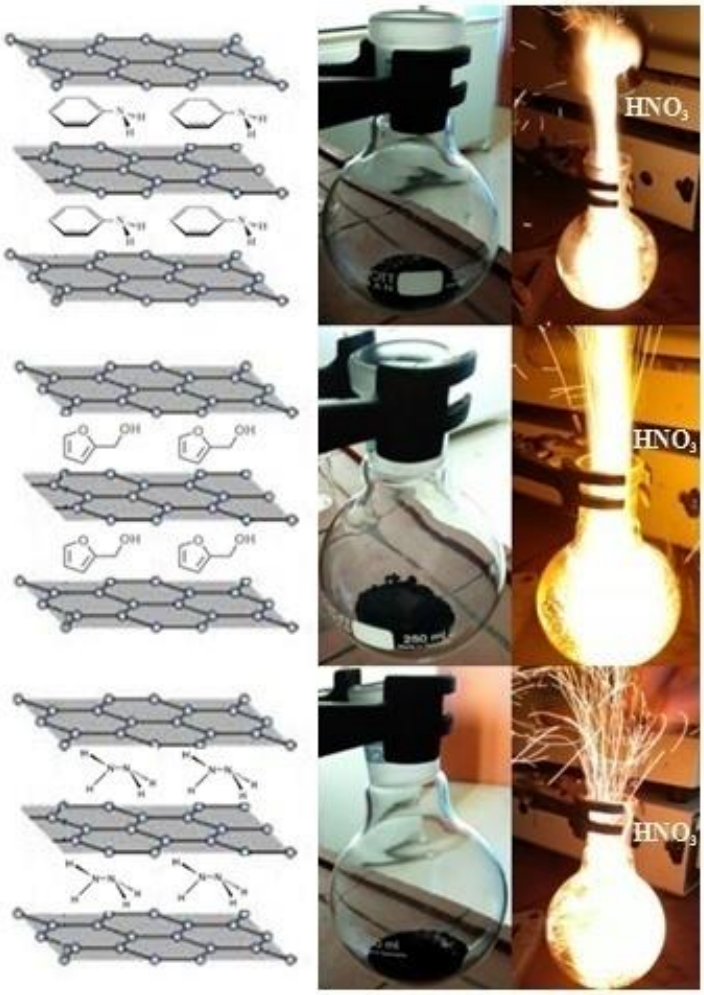

Figure 10: The aniline-, furfuryl alcohol- and hydrazine-intercalated carbons gave fast and bright ignitions upon addition of fuming nitric acid HNO_3.

Lastly, in an effort to demonstrate the propellant properties of the mixtures primarily composed of intercalated carbon adducts and fuming nitric acid HNO_3, we set out to build an improvised mini rocket made of a small glass vial weighing 4.5 g, stuffed with 1 g of aniline-intercalated WTPS and a piece of cotton imbibed with 1 g of the strong oxidizer. Once the glass vial was flipped over, the strong oxidizer slowly wetted the carbon particles to initiate an exothermic reaction that lifted off the glass vial by 1 cm in a cloud of smoke and sparks (Figure 11). Note that the cited photo serves only as a proof of concept based on a rough design. Higher fuel loadings and faster mixing rates of the reagents is expected to give even greater lifts-off.

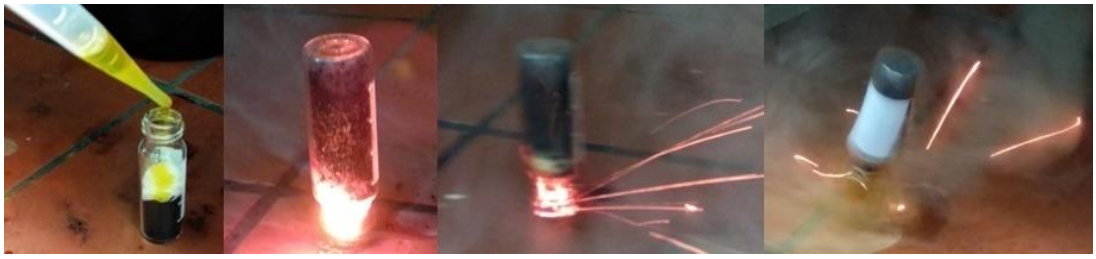

Figure 11: A mini rocket was made of a small glass vial, the aniline-intercalated WTPS and fuming nitric acid HNO_3. The glass vial was partly packed with the solid fuel and a small piece of cotton was placed on top of the black powder. Following, fuming nitric acid HNO_3 was added dropwise until it was fully absorbed by the small piece of cotton. The vial was then flipped upside down to initiate ignition and lift-off the mini rocket within a veil of smoke and sparks.

4. Conclusions

Biomass waste carbonization in piranha solution is a versatile new method for obtaining energetic carbon materials suitable for solid rocket fuels. Besides the cases of stale bread, spent coffee and cardboard biomass wastes presented previously from our group, in this work we have provided another example of biomass waste in this context, aiming to further emphasize the general character of the method. In particular, we have shown here the piranha solution-mediated carbonization of waste tea, the latter globally produced in sizeable amounts every year. Carbonization proceeds fast and exothermically at ambient conditions leading to carbon nanosheets at a good yield of 32 %; the carbon nanosheets are highly amorphous, have a distribution of thicknesses ranging from thinner to thicker sheets, and contain mostly O, N and S structural heteroatoms originating from the parent waste and the piranha solution treatment. Because of its relatively large interlayer spacing (d_{002} = 4.5 Å), the waste tea-derived carbon reacts hypergolically with fuming nitric acid HNO_3 at ambient conditions. Moreover, intercalation with hypergolically active molecules, such as aniline, furfuryl alcohol and hydrazine, can further boost ignition, thus making such energetic carbons appealing candidates for solid fuels in rocket propellant compositions.

Conflict of interest

The authors declared that they have no conflicts of interest to this work.

Acknowledgments

This study was funded by the project "National Infrastructure in Nanotechnology, Advanced Materials and Micro-/Nanoelectronics" (MIS-5002772) which was implemented under the action "Reinforcement of the Research and Innovation Infrastructure", funded by the Operational Programme "Competitiveness, Entrepreneurship and Innovation" (NSRF 2014-2020), and co-financed by Greece and the European Union (European Regional Development Fund). I. T. acknowledges the support by the Operational Programme Research, Development and Education-Project No. CZ.02.1.01/0.0/0.0/15_003/0000416 of the Ministry of Education, Youth and Sports of the Czech Republic. V. Š. acknowledges the support from the Internal Student Grant Agency of the Palacký

University in Olomouc, Czech Republic (IGA_PrF_2022_019). Authors also acknowledge the project Nano4Future reg. no. CZ.02.1.01/0.0/0.0/16_019/0000754 financed from ERDF/ESF. Operation of XPS and TEM facilities were partly funded by the Research Infrastructure NanoEnviCz, supported by the Ministry of Education, Youth and Sports of the Czech Republic under Project No. LM2018124. The authors thank J. Stráská for TEM measurements and J. Kašlík for XRD.

References

1. Rene ER, La DD, Nguyen DD. Emerging technologies for waste biomass to energy: innovations and research challenges. Front Energy Res 9 (2021): 734541.

2. Chalmpes N, Baikousi M, Giousis T, et al. Biomass waste carbonization in piranha solution: a route to hypergolic carbons? Micro 2 (2022): 137-153.

3. Demirbas A. Evaluation of biomass materials as energy sources: upgrading of tea waste by briquetting process. Energy Sources 21 (1999): 215-220.

4. Bansode PA, Khandagale SM, Salunkhe HS, et al. Isolation and characterization of caffeine from waste tea. World J Pharm Res 4 (2015): 585-590.

5. Gao T, Shi Y, Xue Y, et al. Polyphenol extract from superheated steam processed tea waste attenuates the oxidative damage in vivo and in vitro. J Food Biochem 44 (2020): e13096.

6. Khayum N, Murugan SAS. Biogas potential from spent tea waste: a laboratory scale investigation of co-digestion with cow manure. Energy 165 (2018): 760-768.

7. Ahluwalia SS, Goyal D. Removal of heavy metals by waste tea leaves from aqueous solution. Eng Life Sci 5 (2005): 158-162.

8. Hussain S, Anjali KP, Hassan ST, et al. Waste tea as a novel adsorbent: a review. Appl Water Sci 8 (2018): 165.

9. Guo S, Awasthi MK, Wang Y, et al. Current understanding in conversion and application of tea waste biomass: a review. Bioresour Technol 338 (2021): 125530.

10. Eom H, Kim J, Nam I, et al. Recycling black tea waste biomass as activated porous carbon for long life cycle supercapacitor electrodes. Materials 14 (2021): 6592.

11. Ratnaji T, Kennedy LJ. Hierarchical porous carbon derived from tea waste for energy storage applications: waste to worth. Diam Relat Mater 110 (2020): 108100.

12. Ma Q, Xi H, Cui F, et al. Self-templating synthesis of hierarchical porous carbon with multi-heteroatom co-doping from tea waste for high-performance supercapacitor. J Energy Storage 45 (2022): 103509.

13. Chen K, Qing W, Hu W, et al. On-off-on fluorescent carbon dots from waste tea: their properties, antioxidant and selective detection of CrO_4^{2-}, Fe^{3+}, ascorbic acid and L-cysteine in real samples. Spectrochim Acta A Mol Biomol Spectrosc 213 (2019): 228-234.

14. Auta M, Hameed BH. Preparation of waste tea activated carbon using potassium acetate as an activating agent for adsorption of Acid Blue 25 dye. Chem Eng J 171 (2011): 502-509.

15. Li B, Zhang Y, Xu J, et al. Simultaneous carbonization, activation, and magnetization for producing tea waste biochar and its application in

tetracycline removal from the aquatic environment. J Environ Chem Eng 9 (2021): 105324.

16. Chalmpes N, Spyrou K, Bourlinos AB, et al. Synthesis of highly crystalline graphite from spontaneous ignition of in situ derived acetylene and chlorine at ambient conditions. Molecules 25 (2020): 297.

17. Roh JS. Structural study of the activated carbon fiber using laser Raman spectroscopy. Carbon Lett 9 (2008): 127-130.

18. Saikia BK, Boruah RK, Gogoi PK. A X-ray diffraction analysis on graphene layers of Assam coal. J Chem Sci 121 (2009): 103-106.

19. Puech P, Kandara M, Paredes G, et al. Analyzing the Raman spectra of graphenic carbon materials from kerogens to nanotubes: what type of information can be extracted from defect bands? C 5 (2019): 69.

20. Bourlinos AB, Giannelis EP, Sanakis Y, et al. A graphite oxide-like carbogenic material derived from a molecular precursor. Carbon 44 (2006): 1906-1912.

21. Al-Maliki S, AL-Masoudi M. Interactions between mycorrhizal fungi, tea wastes, and algal biomass affecting the microbial community, soil structure, and alleviating of salinity stress in corn yield (*Zea mays* L.). Plants 7 (2018): 63.

22. Chalmpes N, Moschovas D, Tantis I, et al. Carbon nanostructures derived through hypergolic reaction of conductive polymers with fuming nitric acid at ambient conditions. Molecules 26 (2021): 1595.

23. Xie W, Ng KM, Weng LT, et al. Characterization of hydrogenated graphite powder by X-ray photoelectron spectroscopy and time-of-flight secondary ion mass spectrometry. RSC Adv 6 (2016): 80649-80654.

24. Yan Q-L, Gozin M, Zhao F-Q, et al. Highly energetic compositions based on functionalized carbon nanomaterials. Nanoscale 8 (2016): 4799-4851.

25. Bourlinos AB. A new generation of carbon-containing hypergolic fuels based on water-ignitable C-NaH mixtures. J Nanotechnol Res 4 (2022): 1-9.

26. Rastogi RP, Munjal NL. Mechanism and kinetics of pre-ignition reactions: part I-aniline-red fuming nitric acid propellants. Indian J Chem 4 (1966): 463-468.

27. Chalmpes N, Bourlinos AB, Talande S, et al. Nanocarbon from rocket fuel waste: the case of furfuryl alcohol-fuming nitric acid hypergolic pair. Nanomaterials 11 (2021): 1.

28. Jain SR. Self-igniting fuel-oxidizer systems and hybrid rockets. J Sci Ind Res 62 (2003): 293-310.

This article is an open access article distributed under the terms and conditions of the Creative Commons Attribution (CC-BY) license 4.0